

AperTO - Archivio Istituzionale Open Access dell'Università di Torino

**Solid Lipid Nanoparticles for Potential Doxorubicin  
Delivery in Glioblastoma Treatment: Preliminary In Vitro Studies.**

**This is the author's manuscript**

*Original Citation:*

*Availability:*

This version is available <http://hdl.handle.net/2318/145777> since 2016-07-14T13:10:09Z

*Published version:*

DOI:10.1002/jps.24002

*Terms of use:*

Open Access

Anyone can freely access the full text of works made available as "Open Access". Works made available under a Creative Commons license can be used according to the terms and conditions of said license. Use of all other works requires consent of the right holder (author or publisher) if not exempted from copyright protection by the applicable law.

(Article begins on next page)



# UNIVERSITÀ DEGLI STUDI DI TORINO

***This is an author version of the contribution published on:***

*Questa è la versione dell'autore dell'opera:*

[J Pharm Sci, 103(7):2157-65. 2014, doi: 10.1002/jps.24002]

***The definitive version is available at:***

*La versione definitiva è disponibile alla URL:*

[<http://onlinelibrary.wiley.com>]

# Solid Lipid Nanoparticles for Potential Doxorubicin Delivery in Glioblastoma Treatment: Preliminary *In Vitro* Studies

LUIGI BATTAGLIA,<sup>1</sup> MARINA GALLARATE,<sup>1</sup> ELENA PEIRA,<sup>1</sup> DANIELA CHIRIO,<sup>1</sup> ELISABETTA MUNTONI,<sup>1</sup> ELENA BIASIBETTI,<sup>2</sup> MARIA TERESA CAPUCCHIO,<sup>2</sup> ALBERTO VALAZZA,<sup>2</sup> PIER PAOLO PANCIANI,<sup>3</sup> MICHELE LANOTTE,<sup>3</sup> DAVIDE SCHIFFER,<sup>4</sup> LAURA ANNOVAZZI,<sup>4</sup> VALENTINA CALDERA,<sup>4</sup> MARTA MELLAI,<sup>4</sup> CHIARA RIGANTI<sup>5</sup>

<sup>1</sup> Università degli Studi di Torino, Dipartimento di Scienza e Tecnologia del Farmaco, Torino, Italy

<sup>2</sup> Università degli Studi di Torino, Dipartimento di Scienze Veterinarie, Grugliasco, Italy

<sup>3</sup> Università degli Studi di Torino, Dipartimento di Neuroscienze, Torino, Italy

<sup>4</sup> Centro di NeuroBioOncologia, Policlinico di Monza, Vercelli, Italy

<sup>5</sup> Università degli Studi di Torino, Dipartimento di Oncologia, Orbassano, Ital

## Abstract

The major obstacle to glioblastoma pharmacological therapy is the overcoming of the blood–brain barrier (BBB). In literature, several strategies have been proposed to overcome the BBB: in this experimental work, solid lipid nanoparticles (SLN), prepared according to fatty acid coacervation technique, are proposed as the vehicle for doxorubicin (Dox), to enhance its permeation through an artificial model of BBB. The *in vitro* cytotoxicity of Dox-loaded SLN has been measured on three different commercial and patient-derived glioma cell lines. Dox was entrapped within SLN thanks to hydrophobic ion pairing with negatively charged surfactants, used as counterions. Results indicate that Dox entrapped in SLN maintains its cytotoxic activity toward glioma cell lines; moreover, its permeation through hCMEC/D3 cell monolayer, assumed as a model of the BBB, was increased when the drug was entrapped in SLN. In conclusion, SLN proved to be a promising vehicle for the delivery of Dox to the brain in glioblastoma treatment. © 2014 Wiley Periodicals, Inc. and the American Pharmacists Association J Pharm Sci 103:2157–2165, 2014

Enhanced Article Feedback

## INTRODUCTION

The blood–brain barrier (BBB) is the main obstacle hampering the transport of most drugs from the blood into the brain. BBB, formed by the endothelial cells of the cerebral capillaries, comprises the major exchange interface between the blood and the brain[1, 2] and, in addition to tight junctions, BBB is rich—on the luminal surface—of efflux membrane transporters such as P-glycoprotein (Pgp) and multidrug resistance-related proteins (MRPs),[3] which recognize various anticancer drugs as substrates.

In literature, several strategies have been proposed to overcome this barrier aimed to improve drug delivery into the brain, including osmotic opening of the tight junctions[4] and the direct surgical

administration of drugs into the brain. The application of nanotechnology by using liposomes and nanoparticles seems to be one of the most promising approaches.[5, 6]

Malignant brain tumor chemotherapy is very difficult because the blood–tumor barrier (BTB) limits the amount of potent agents that can be delivered to the tumor, resulting in the lack of ability of the drug to reach a therapeutic level. Although BTB is in itself is more permeable than BBB, therapeutics are rarely effective in patients with brain tumors because the selective permeability of BTB still blocks many antitumor agents and stops them approaching their target.[7] Glioblastoma multiforme is one of the most common forms of glioma whose pharmacotherapy is adjuvant and therefore rarely applied in first instance[8]: generally, it follows surgery and is subsequent or contemporaneous with radiotherapy. It is directed mainly toward the eradication of residual tumor cells after surgery or radiotherapy. This cell population includes those cells that migrated from the tumor into healthy tissue (and that were not destroyed by previous treatment) or that feed the tumor from far sites, still active[9] and is hard to treat completely by surgical resection because of the diffuse nature of the glioma. As a result, residual microscopic tumor cells usually need to be eliminated by additional chemotherapy or radiotherapy. Even patients who are optimally treated with combined multimodal treatments have a median survival of only 12 months.

A possibility to deliver drugs to the central nervous system (CNS) is the use of polymeric nanoparticles.[10] The ability of these carriers to overcome BBB and to produce biologic effects on the CNS was shown in a number of studies. Over the last few years, progress in the understanding of the mechanism of nanoparticle uptake into the brain suggests that receptor-mediated endocytosis in brain capillary endothelial could be the most probable mechanism. Modification of the nanoparticle surface with covalently attached targeting ligands or by coating with certain surfactants enabling the adsorption of specific plasma proteins are necessary for this receptor-mediated uptake.[11]

Solid lipid nanoparticles (SLN) are disperse systems with mean diameters ranging between 50 and 1000 nm and represent an alternative to polymeric particulate carriers. The main advantage of lipid carriers in drug delivery is the use of physiological or biocompatible lipids or lipid molecules with a history of safe use in therapy.[12] Several SLN production methods are described in literature: cold and hot homogenization,[13] microemulsion dilution,[14] microemulsion cooling,[15] solvent evaporation,[16] solvent injection,[17] and emulsification diffusion technique with low-toxicity solvents.[18-20]

Recently, in our research group, a new solvent-free technique was developed to produce SLN of fatty acids by acidification of a micellar solution of their alkaline salts.[21] As pH is lowered, fatty acids precipitate owing to proton exchange between the acid solution and the alkaline salt: this process can be defined as “coacervation.” With this technique, lipophilic drugs can be entrapped within nanoparticles by allowing their dissolution in micellar solution prior to acidification. It has also been demonstrated that hydrophilic molecules can effectively be entrapped in SLN enhancing their lipophilicity by hydrophobic ion pairing (HIP): indeed, a cytotoxic hydrophilic molecule, cisplatin, has been carried in SLN by forming a drug–surfactant complex.[22] Such strategy was also successfully used for peptide drugs entrapment in SLN.[23]

In literature, several studies are reported on the entrapment of antineoplastic drugs in SLN and the consequent increase of their both chemico-physical stability and cytotoxicity on tumor cell lines.[24] SLN can be internalized in cells through simple or carrier-mediated endocytosis or phagocytosis[25] owing to particle surface charges. Recent studies show that SLN can be uptaken by cells without altering their morphological and metabolic characteristics.[26]

Doxorubicin (Dox) is a potent, broad spectrum chemotherapeutic drug used around the world. In its unaltered form, Dox has shown great treatment potential, being regarded as one of the most potent chemotherapeutic drugs and having been used for treating cancer for over 30 years.[27] The ability to combat rapidly dividing cells and to slow disease progression has been widely acknowledged for several decades, limited only by its toxicity on noncancerous cells in the human body. Dox causes toxicity to most major organs, especially life-threatening cardiotoxicity, which forces the treatment to become dose limiting.

Over the years, many studies have been conducted to devise a drug delivery system that would eliminate these adverse effects including liposomes and nanoparticulate systems.[28, 29]

The aim of the present work is to obtain Dox-loaded SLN as possible drug delivery systems for intravenous administration and to evaluate their capacity *in vitro* to overcome BBB and their cytotoxicity against primary human glioblastoma cells. Because of the hydrophilic nature of Dox that hampers its entrapment in SLN, several lipophilic counterions are screened to perform lipophilic ion pairing of the drug.

## **EXPERIMENTAL**

### **Materials**

Doxorubicin hydrochloride was a kind gift from Farmitalia (Milan, Italy). Sodium dioctylsulfosuccinate (AOT) and hydrochloric acid were obtained from Merck (Darmstadt, Germany). Citric acid, phosphoric acid, lactic acid, and sodium dihydrogenphosphate were obtained from A.C.E.F. (Fiorenzuola d'Arda, Italy). Eighty percent hydrolyzed PVA 9000–10,000 Mw (PVA 9000) and sodium taurodeoxycholate (TDC) were obtained from Sigma (Dorset, UK). Sodium stearate, sodium palmitate, and sodium decansulfonate (SDeS) were obtained from Fluka (Buchs, Switzerland). Sodium arachidate (SAr) and sodium behenate were obtained from Nu-Chek (Elysian, Minnesota).

Deionized water was obtained by a MilliQ<sup>®</sup> system (Millipore, Bedford, Missouri). All other chemicals were analytical grade and used without any further purification.

### **Methods**

#### **Ion Pair Preparation**

Hydrophobic ion pairs between Dox and each counterion (AOT, TDC, and SDeS) were prepared according to literature methods.[30]

Doxorubicin hydrochloride (5 mg/mL) was dissolved in water and an appropriate volume of each counterion aqueous solution was added to obtain 1:1 drug–counterion molar ratio, except for SDeS, which was added at a 1:3 drug–counterion molar ratio.

The obtained precipitates were centrifuged at 55,000g (Allegra R64 centrifuge; Beckmann Coulter s.r.l. Cassina De' Pecchi - Milano, Italia), washed with deionized water, and then dried for 24 h.

#### **Ion Pair Characterization**

A weighted amount of the freeze-dried product was dissolved in ethanol (dimethyl sulfoxide for SDeS–Dox ion pair) to obtain a stock solution of 14 mg/mL Dox concentration (supposing a 1:1 Dox—counterion molar ratio). The actual molar ratio of the precipitated ion pair was confirmed after 1:300 dilution in ethanol of the stock solution and HPLC analysis of Dox content.

To determine ion-pair aqueous solubility, a weighted amount of the freeze-dried ion pair was suspended in 1 mL water and kept under stirring for 1 h: the obtained suspension was then centrifuged at 55,000 *g* (Allegra R64 centrifuge; Beckmann Coulter) and the supernatant analyzed by HPLC.

Ion pairs partition coefficient was calculated by dissolving a known amount of Dox hydrochloride in water (10 µg/mL) and adding an aqueous counterion solution at a 1:1 drug–counterion molar ratio, except for SDeS, which was added at a 1:3 drug–counterion molar ratio. The aqueous phase was shaken for 1 min with an equal volume of octanol in a separator funnel, then the mixture was allowed to settle. Ion-pair partition coefficient was calculated determining its aqueous concentration by HPLC before and after partitioning with octanol.

### **SLN Preparation**

Different operative conditions were used for SLN preparation according to the fatty acid under study (palmitic acid, PA; stearic acid, SA; arachidic acid, AA; behenic acid, BA). Fatty acid sodium salt was dispersed in the PVA 9000 solution and the mixture was then heated under stirring (300 rpm) just above the Krafft point of fatty acid sodium salt to obtain a clear solution. A selected acidifying solution (coacervating solution) was then added dropwise.[21] The obtained suspension was then cooled in an ice bath under stirring at 300 rpm. For Dox-loaded SLN, Dox ion pair was added to the micellar solution prior to acidification, dissolved in ethanol (dimethyl sulfoxide for SDeS–Dox ion pair).

### **SLN Characterization**

Solid lipid nanoparticles particle size distribution was determined by the laser light scattering technique (Brookhaven, Long Island, New York). The dispersions were diluted with water (1:1000) and measurements were carried out at an angle of 90° with a laser beam of 675 nm.

Drug entrapment efficiency (EE%) was calculated as the ratio between the amount of drug entrapped within the lipid matrix and the amount used to prepare SLN. The entrapped drug was determined as follows: 1 mL SLN suspension was centrifuged for 15 min at 55,000*g* and the precipitate was washed twice with 1 mL 30:70 ethanol–water to remove adsorbed drug. The solid residue was dissolved in 1 mL ethanol, 0.5 mL water was then added to precipitate the lipid matrix, and the supernatant obtained was injected in HPLC for drug quantification.

The lipid fraction was selectively precipitated by diluting in HPLC mobile phase, and the supernatant was centrifuged and analyzed by HPLC.

### **Dox In Vitro Release in Normal Saline**

The release of Dox in normal saline from SLN was studied by using rotating cells. An aliquot (2 mL) of Dox–AOT BA SLN was placed in the donor compartment, whereas the receptor compartment contained 2 mL of normal saline. Dox hydrochloride aqueous solution was used as blank.

The dialysis membrane (12,000–14,000 Da cutoff; Visking) was placed between the two compartments. At fixed 2-h intervals, the receptor phase was withdrawn, replaced with fresh normal saline, and spectrophotometrically analyzed ( $\lambda = 480$  nm).

In all samples under study, Dox concentration was 280  $\mu\text{g/mL}$ .

### **Dox In Vitro Release with the Test Tube Assay**

To assess the entrapment of ion pairs within SLN, Dox release studies were performed using a test tube assay, as described in literature[31]: decanol was used as organic receiving phase. In total, 5 mL decanol was layered onto the surface of 5 mL Dox–AOT-loaded SLN and the system was kept under mild stirring (50 rpm); at scheduled times, a small amount of the receiving phase was withdrawn and the supernatant analyzed spectrophotometrically ( $\lambda = 480$  nm) for Dox determination. Ion-pair aqueous suspensions in the absence of SLN were used as blanks. In all samples under study, Dox concentration was 280  $\mu\text{g/mL}$ .

### **Cell Culture**

hCMEC/D3 cells, a primary human brain microvascular endothelial cell line that retains the property of BBB *in vitro*, were cultured as reported[32] and were seeded at 50,000/cm<sup>2</sup> and grown for 7 days up to confluence in Petri dishes and Transwell devices (0.4  $\mu\text{m}$  diameter pores-size; Corning Life Sciences, Chorges, France). Permeability coefficients of dextran–fluorescein isothiocyanate (FITC), [<sup>14</sup>C]-sucrose (589 mCi/mmol; PerkinElmer, Waltham, Massachusetts), [<sup>14</sup>C]-inulin (10 mCi/mmol; PerkinElmer), taken as a parameter of paracellular transport across hCMEC/D3 monolayer,[33] were measured as previously reported,[34] and were equal to:  $0.013 \pm 0.002 \times 10^{-3}$  cm/min for dextran–FITC ( $n = 3$ );  $1.31 \pm 0.24 \times 10^{-3}$  cm/min for [<sup>14</sup>C]-sucrose ( $n = 3$ );  $0.51 \pm 0.08 \times 10^{-3}$  cm/min for [<sup>14</sup>C]-inulin ( $n = 3$ ), in line with previous literature. [34] Transendothelial electrical resistance value for hCMEC/D3 cells was between 30 and 40  $\Omega \times \text{cm}^2$ . [35]

Primary human glioblastoma cells (CV17, 01010627) were obtained from surgical samples of patients operated at the Department of Neuroscience, Neurosurgical Unit, University of Turin, Italy. The histological diagnosis was performed according to WHO guidelines. Cells were propagated in Dulbecco's modified Eagle's medium, supplemented with 1% (v/v) penicillin-streptomycin and 10% (v/v) fetal bovine serum. U87-MG cells (ATCC, Rockville, Maryland) were used as glioblastoma reference cell line.

In coculture experiments, 500,000 glioblastoma cells were added in the lower chamber of Transwells 4 days after seeding hCMEC/D3 cells in the upper chamber of Transwells. After 3 days of coculture, the medium of the upper chamber was replaced with fresh medium, with or without free Dox or SLN-entrapped Dox–AOT, as detailed under *Results*.

### **In Vitro Cytotoxicity on BBB Cells**

The early signs of cytotoxicity of Dox, blank SLN, or SLN-entrapped Dox–AOT on hCMEC/D3 monolayer were verified as follows.

The extracellular medium was centrifuged at 12,000g for 15 min to pellet cellular debris, whereas cells were washed with fresh medium, detached with trypsin–ethylenediaminetetraacetic acid (0.05/0.02% v/v), resuspended in 0.2 mL of 82.3 mmol/L triethanolamine phosphate–HCl (pH 7.6) and sonicated on ice with two 10 s bursts (Labsonic sonicator, 100 W). Lactate dehydrogenase

(LDH) activity was measured in the extracellular medium and in the cell lysate: 50  $\mu$ L of supernatant from extracellular medium or 5  $\mu$ L of cell lysate were incubated at 37°C with 5 mmol/L NADH. The reaction was started by adding 20 mmol/L pyruvic acid and was followed for 6 min, measuring absorbance at 340 nm with Packard EL340 microplate reader (Bio-Tek Instruments, Winooski, Vermont). The reaction kinetics was linear throughout the time of measurement. Both intracellular and extracellular enzyme activity were expressed in  $\mu$ mol NADH oxidized per minute per dish, and then extracellular LDH activity was calculated as percentage of the total LDH activity in the dish.

### **Permeability of Dox Through hCMEC/D3 Cell Monolayer**

hCMEC/D3 cells, seeded as reported above in Transwell devices, were incubated at day 7 with free Dox or SLN-entrapped Dox–AOT, at the experimental conditions described in the *Results* section. The medium in lower chamber was then collected and Dox amount was measured fluorimetrically, using a LS-5 spectrofluorimeter (PerkinElmer). Excitation and emission wavelengths were 475 and 550 nm, respectively. Fluorescence was converted in nmol Dox per  $\text{cm}^2$ , using a calibration curve previously set. The permeability coefficients were calculated as described.[36]

In coculture experiments, Dox was added in the upper chamber of Transwell device; after 3 h, the insert was removed and a 50- $\mu$ L aliquot of the medium in the lower chamber was collected and diluted 1:10 into ethanol–HCl 0.3 N [1:1 (v/v) solution). The amount of Dox was measured fluorimetrically as reported above. Fluorescence was converted into nmol/mL according to a titration curve previously set.

### **Uptake of Dox Within hCMEC/D3 Cell**

hCMEC/D3 cells, seeded in 35-mm diameter Petri dishes, were grown up to the confluence for 7 days and then incubated for 3 h with 0.1 and 1  $\mu$ M of free Dox or SLN-entrapped Dox–AOT. At the end of the incubation time, cells were washed twice with phosphate-buffered saline (PBS), detached with trypsin–ethylenediaminetetraacetic acid, centrifuged at 27.000 g for 2 min, resuspended in 0.5 mL ethanol–HCl 0.3 N [1:1 (v/v) solution] and sonicated. A 50- $\mu$ L aliquot was used to measure the protein content; the remaining part was used to measure the intracellular content of Dox, as detailed above. Fluorescence was converted in nmol Dox per milligram cell prot, using a calibration curve previously set.

### **Glioblastoma Cell Viability**

To measure the viability of glioblastoma cells cultured alone or cocultured with hCMEC/D3 cells, cells were treated as detailed under *Results*, and then incubated for 1 h at 37°C in culture medium containing 70  $\mu$ g/mL of Neutral Red solution (Sigma). Cells were washed three times with PBS and rinsed with stop buffer [32 mM trisodium citrate, 50% (v/v) methanol; pH 6]. The absorbance at 540 nm was read using a Synergy HT Multi-Detection Microplate Reader (Bio-Tek). The absorbance of untreated cells was considered as 100% viability and the results were expressed as percentage of viable cells versus untreated cells.

### **Dox HPLC Analysis**

Experimental conditions were as follows: YL9110 quaternary pump (Young Lin, Hogue-dong, Anyang, Korea) equipped with a Merck-Hitachi L 4200 UV-visible lamp (Merck-Hitachi, Tokyo, Japan); column: HiQ sil C18HS 150  $\times$  4.6  $\text{mm}^2$  (KIA-technologies, Kyoto, Japan); mobile phase:  $\text{CH}_3\text{OH}/\text{H}_2\text{O}$  [containing 0.1% anhydrous formic acid and 0.1%, ammonia solution (25%) to pH



3.0] 60/40; flow: 1 mL/min; detection  $\lambda = 480$  nm; integration with YL-Clarity (Young Lin); retention time: 8.0 min[38].

## RESULTS

Hydrophobic ion pairs between Dox and counterions (AOT, TDC, and SDeS) were obtained by simply mixing aqueous solutions of drug and counterion: the ion pair precipitates in water as red precipitate. The actual molar ratio between counterions and Dox measured by HPLC analysis on the weighted precipitate is 1:1. Ion pair water solubility and partition coefficient are reported in Table 1. It should be noted that the highest partition coefficient was that obtained with Dox–AOT ion pair as it was increased more than 100 times compared with free Dox. For this reason, further *in vitro* studies were conducted on Dox–AOT ion pair.

Table 1. Solubility and Partition Coefficient of Dox Ion Pairs

**Counterion Solubility ( $\mu\text{g/mL}$ ) Log  $P$**

-	Not Determined	-0.73
AOT	50	1.29
TDC	250	0.62
SDeS	19	1.13

Compositions and mean diameters of blank SLN prepared according to the coacervation method are reported in Table 2. Dox-loaded SLN were prepared by adding 200  $\mu\text{L}$  of Dox–HIP stock solution (corresponding to 2.8 mg Dox) to 10 mL of micellar solution prior to acidification. In a preliminary experiment, Dox-loaded BA–SLN was prepared using different ion pairs: their mean particle size and different Dox–HIP EE% values are reported in Table 3.

Table 2. Blank SLN Composition

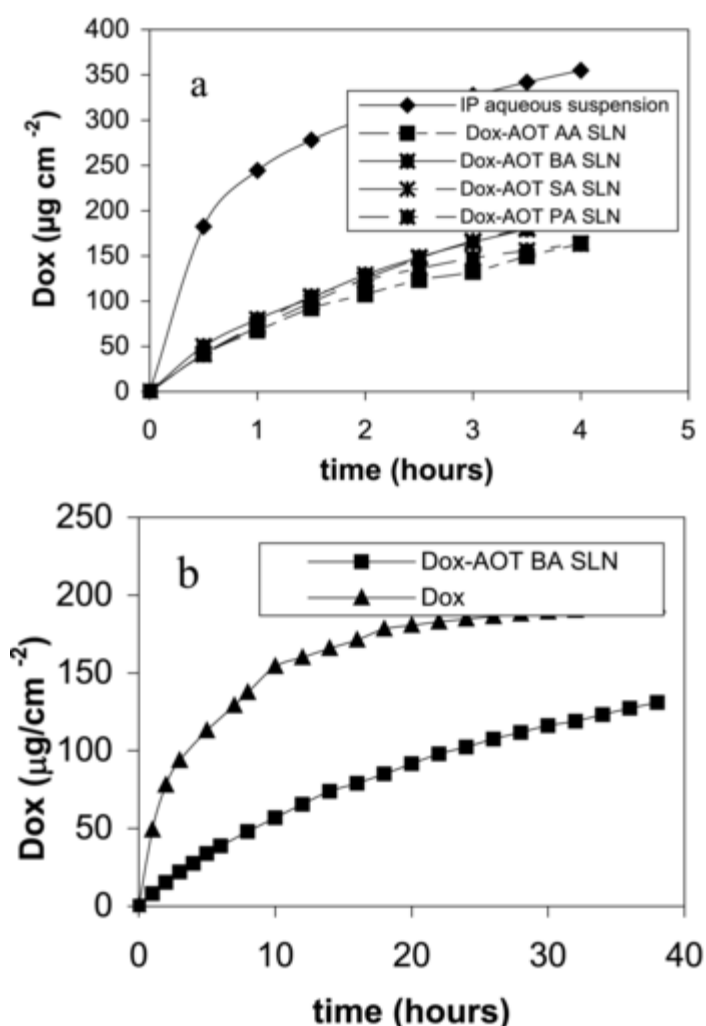
	PA–SLN	SA–SLN	AA–SLN	BA–SLN
1. <sup>a</sup>				
Corresponding to 100 mg fatty acid.				
SM				
Sodium palmitate	108 mga			
Sodium stearate		107 mga		
SAr			107 mga	
Sodium behenate				106 mga
PVA 9000 (mg)	100	100	200	200
1 M citric acid	0.2 mg			
1 M $\text{Na}_2\text{HPO}_4$				
1 M lactic acid		0.5 mL		
1 M $\text{NaH}_2\text{PO}_4$			0.2 mL	0.2 mL
1 M $\text{H}_3\text{PO}_4$			0.3 mL	
1 M HCl				0.3 mL
Water (mL)	9.8	9.5	9.5	9.5
Mean diameter (nm)	$278 \pm 25$	$289 \pm 16$	$303 \pm 20$	$305 \pm 30$
Polydispersity	0.05	0.101	0.15	0.12

Table 3. Mean Particle Size and EE% of PA, SA, BA, AA–SLN-loaded with Different Dox Ion Pairs

<b>Fatty Acid</b>	<b>Counterion</b>	<b>Mean Diameter (nm)</b>	<b>Polidispersity</b>	<b>EE%</b>
BA	TDC	1602 ± 85	0.366	52.1 ± 5.5
BA	SDeS	436 ± 25	0.229	40.0 ± 3.5
BA	AOT	278 ± 10	0.104	78.9 ± 7.3
PA	AOT	391 ± 19	0.128	76.2 ± 5.9
SA	AOT	356 ± 23	0.100	74.3 ± 8.4
AA	AOT	291 ± 15	0.088	74.9 ± 6.3

As it can be noticed, the highest EE% was obtained with AOT as a counterion: consequently, Dox–AOT was chosen to be loaded also in SLN composed of different lipid matrixes. The results obtained in terms of EE% and mean particle size are reported in Table 3, too.

Solid lipid nanoparticles showed a good EE%, regardless of the lipid matrix used. To verify the effective entrapment of Dox–AOT within SLN, drug release was studied. Indeed, the entrapment of the ion pair in the solid lipid matrix, with its subsequent immobilization, should reduce its release rate.[37] In Figure 1a, Dox-release profiles expressed as drug amount per unit area versus time from SLN suspensions in the test tube assay are shown. This method involved two steps: the release of the drug from SLN to the aqueous outer phase and the migration to the organic phase, where it favorably partitions because of the lipophilicity of the ion pair. Despite the partition step in a nonphysiological medium, this assay is suitable to obtain complete release in a few hours, because the organic phase can easily dissolve a lipophilic molecule or complex. When the ion pair is entrapped within the lipid matrix, drug release to the organic phase is slower than that of free ion pair, probably because of the interactions between the lipid matrix and the ion pair. This confirms drug entrapment within SLN, which can reduce drug release rate. Consequently, the amount of Dox released after 4 h from SLN of different lipid matrixes is lower than that from free ion pair (HIP aqueous suspension). Release experiments were performed up to 4 h for comparative purposes, even if further release can be obtained at longer times (data not shown). This experiment does not simulate Dox-IP release in a physiological medium, as the amount of Dox-IP diffusing from SLN to the aqueous phase is continuously removed by the decanol organic phase in which it is more soluble. The experiment represents only an indirect method to confirm Dox-IP entrapment within SLN.



**Figure 1.**

- [Open in figure viewer](#)
- [Download Powerpoint slide](#)

(a) Dox release in the test tube assay. (b) Dox diffusion rate profiles in normal saline.

In Figure 1b, Dox-release profiles expressed as drug amount per unit area versus time in normal saline are shown. The diffusion rate is quite faster when Dox is present in aqueous solution, as more than 70% of the initial Dox amount diffused over 40 h than when entrapped in SLN as an ion pair (less than 30%). This suggests that Dox is actually entrapped in SLN, as the lipid matrix lowers the rate of its release from SLN over a relatively long period of time.

As no relevant differences were recovered in Dox EE% and in mean diameters among the different lipid matrixes tested, two lipid matrixes (the former with short and the latter with long hydrocarbon chain) were chosen for *in vitro* studies on cells. Blank PA and BA SLN were selected to test the biocompatibility of the lipid matrix with the hCMEC/D3 cells, and to perform further permeation studies on hCMEC/D3 cells monolayer. Obtained results after 24-h incubation at four different SLN dilutions [0.1%, 0.01%, 0.001%, 0.0001% (v/v) lipid concentration] are shown in Figure 2. A PA-SLN dose-dependent increase of cytotoxicity can be noted, whereas BA-SLN did not cause any detectable cytotoxicity against hCMEC/D3 cells: as a consequence, BA-SLN were selected for the prosecution of the experimental study.

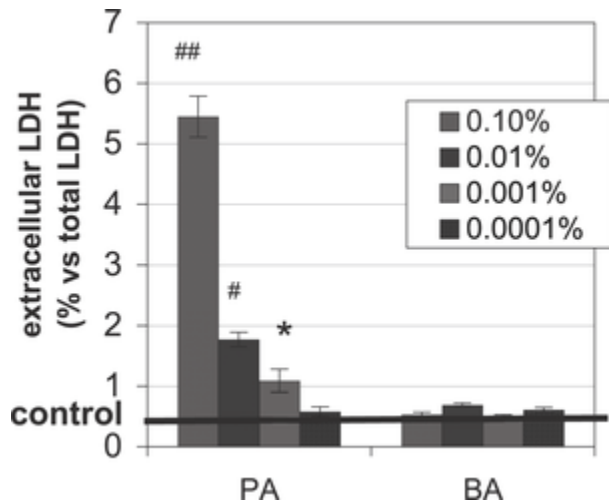


**Figure 2.**

- [Open in figure viewer](#)
- [Download Powerpoint slide](#)

Cytotoxicity of blank PA-SLN and BA-SLN at different lipid concentrations against hCMEC/D3 cells. Significance versus untreated cells (CTRL): \*  $p < 0.05$ ; \*\*  $p < 0.02$ ; #  $p < 0.005$ ; ##  $p < 0.001$  ( $n = 3$ ).

Cytotoxicity of Dox-AOT loaded BA-SLN on hCMEC/D3 cells was then tested in a time-dependent experiment: free Dox was used as a reference at the same concentration present in SLN [1, 0.1, and 0.01  $\mu\text{M}$  Dox, corresponding to 0.1%, 0.01%, and 0.001% (v/v) lipid concentration, respectively]. As it can be noticed from Figure 3, no relevant cytotoxicity of Dox-AOT-loaded BA-SLN and of free Dox was revealed (compared with the control) after 24-h incubation at the three concentrations tested. After 48 and 72 h, on the contrary, a dose-dependent cytotoxicity was present for Dox and Dox-AOT-loaded BA-SLN. To avoid the assays to be performed on a damaged BBB monolayer, permeation experiments through hCMEC/D3 cells were performed after 24-h incubation with the tested formulations (free Dox and Dox-AOT-loaded BA-SLN).

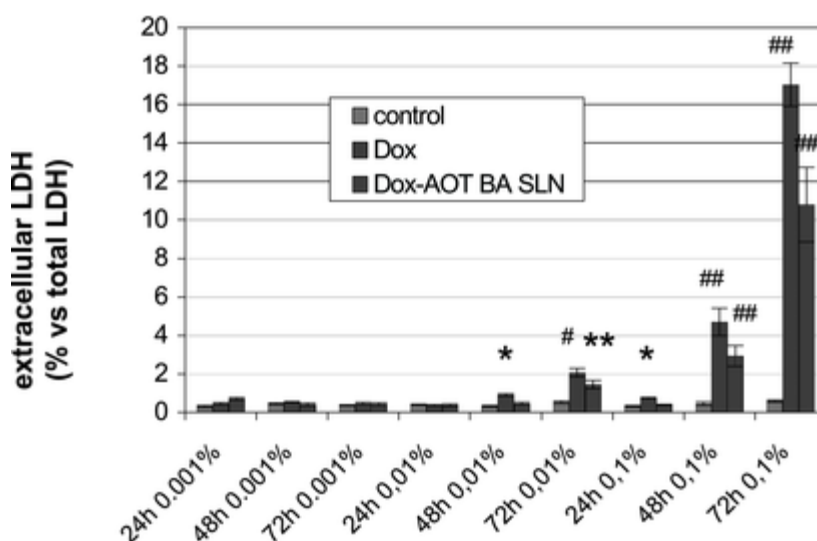


**Figure 3.**

- Open in figure viewer
- Download Powerpoint slide

Cytotoxicity of Dox and Dox–AOT-loaded BA-SLN against hCMEC/D3 cells at 24, 48, and 72 h at different lipid concentrations. Significance versus untreated cells (CTRL): \*  $p < 0.02$ ; \*\*  $p < 0.005$ ; #  $p < 0.002$ ; ##  $p < 0.001$  ( $n = 3$ ).

Permeation experiments through hCMEC/D3 cells monolayer were performed by using two different concentrations of Dox [1 and 0.1  $\mu\text{M}$ , corresponding to 0.1% and 0.01% (v/v) lipid concentration, respectively]: Dox–AOT-loaded BA–SLN and free Dox were compared. As shown in Figure 4, the entrapment in SLN causes an increase in Dox permeation, compared with that of the free drug. Such increase is time and dose dependent. The uptake of Dox by hCMEC/D3 cells was evaluated by measuring the intracellular amount of the drug after 3-h incubation with Dox or Dox–AOT BA–SLN (1 or 0.1  $\mu\text{M}$ ): at 0.1  $\mu\text{M}$ , the amount of intracellular Dox did not significantly differ between free Dox or Dox–AOT BA–SLN. By contrast, at 1  $\mu\text{M}$ , the amount of Dox obtained with Dox–AOT BA–SLN was significantly higher. Moreover, intracellular drug uptake increased in a dose-dependent manner with Dox–AOT BA–SLN, but did not change with free Dox (Fig. 5).

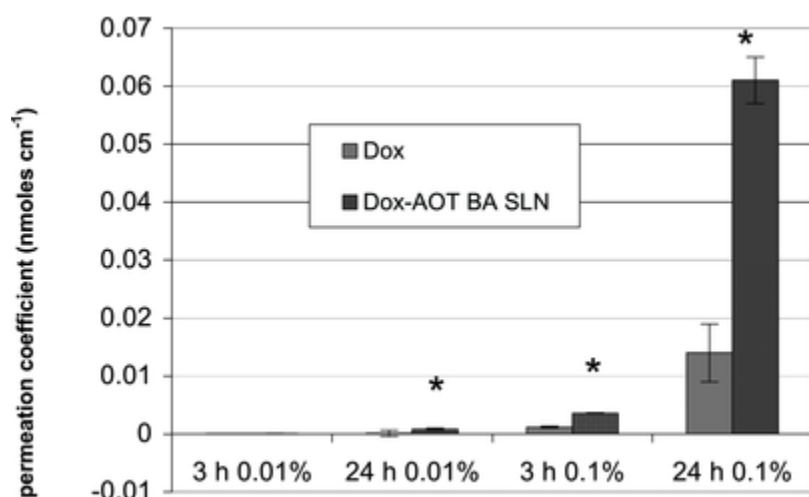


**Figure 4.**

- Open in figure viewer
- Download Powerpoint slide

Dox permeation through hCMEC/D3 cell monolayer from Dox aqueous solution and from Dox–AOT BA–SLN at 0.1 and 1  $\mu\text{M}$  Dox concentration after 3 and 24 h. Significance versus Dox: \*  $p < 0.002$ ; \*\*  $p < 0.001$  ( $n = 3$ ).

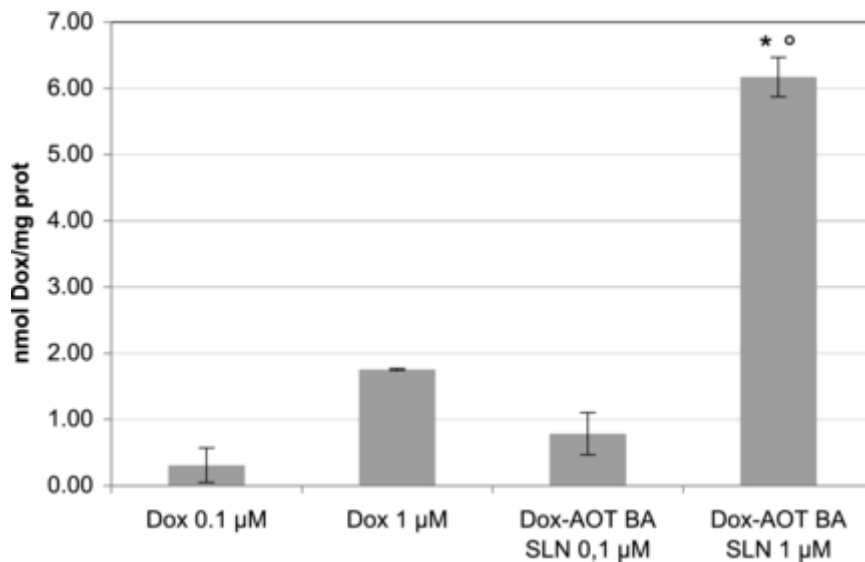


**Figure 5.**

- [Open in figure viewer](#)
- [Download Powerpoint slide](#)

Dox uptake within hCMEC/D3 cells from Dox aqueous solution and from Dox–AOT BA–SLN at 0.1 and 1 µM Dox concentration after 3 h. 0.1 µM concentration versus 1 µM concentration:  $p < 0.01$ ; Dox–AOT versus Dox:  $^{\circ}p < 0.005$  ( $n = 3$ ).

Cytotoxicity of Dox–AOT-loaded BA–SLN was then tested on three different human glioblastoma cell cultures, the U87-MG cell line and the primary human glioblastoma cells CV17 and 01010627. As it can be observed from Figure 6, the entrapment in SLN did not reduce the cytotoxicity of Dox over a wide range of concentrations.

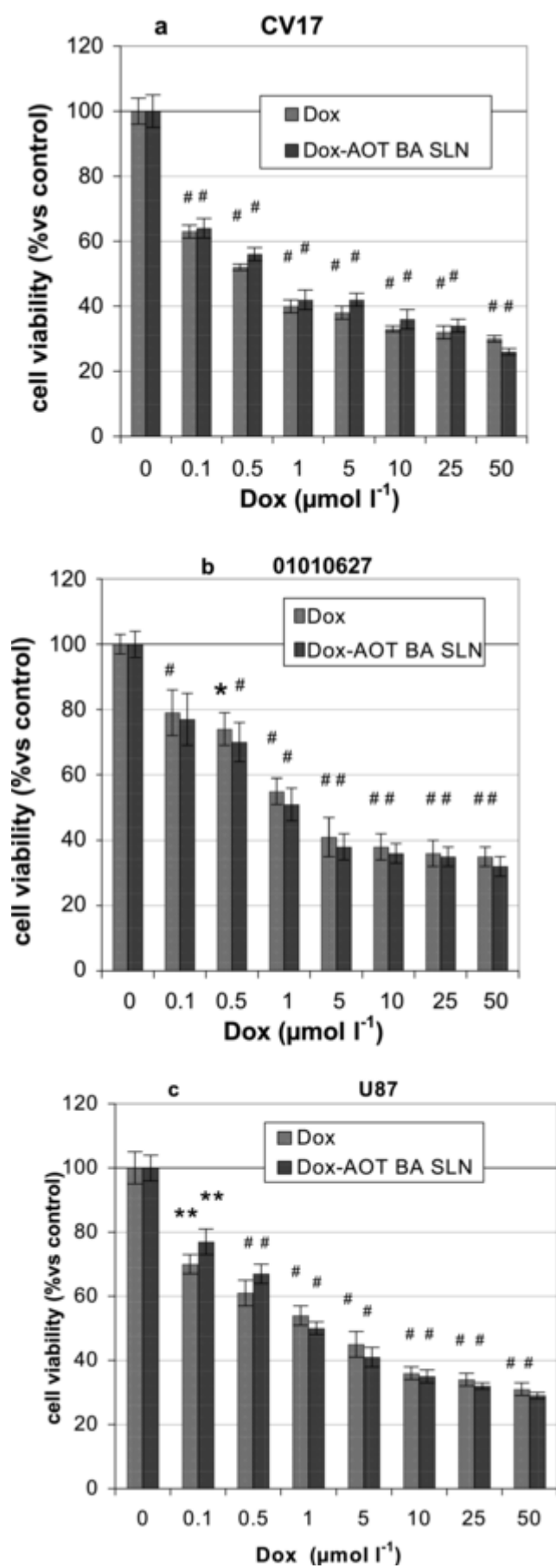


Figure 6.

- Open in figure viewer
- Download Powerpoint slide

Cytotoxicity of Dox–AOT-loaded BA–SLN and free Dox on three human glioma cell lines: *a*, CV17; *b*, 01010627; *c*, U87. Significance versus untreated cells (CTRL): \*  $p < 0.05$ ; \*\*  $p < 0.02$ ; #  $p < 0.001$  ( $n = 4$ ).

Basing on these preliminary data, a coculture experiment was performed, in which hCMEC/D3 cells were grown on the filter of the upper chamber of the Transwell devices and glioma cells were grown in the lower chamber: free Dox and Dox–AOT-loaded BA–SLN were added in the upper chamber and the cytotoxicity exerted by Dox permeated through hCMEC/D3 on glioma cells was evaluated. Dox concentrations used for this experiment were chosen on the basis of the results of Figure 5: indeed, the Dox concentration, which was able to kill at least 50% of the cells, was nearly 5  $\mu\text{M}$  for the various glioma cell lines. This means that concentrations higher than 5  $\mu\text{M}$  should be used in coculture experiments to detect an appreciable damage on glioma cells, as only a very low fraction of free Dox is expected to permeate the hCMEC/D3 cells monolayer.[38] For this reason, 50, 250, 500  $\mu\text{M}$  Dox were used. To avoid cytotoxicity on hCMEC/D3 cells, free Dox and Dox–AOT-loaded BA–SLN were added for 3 h in the upper chamber; the insert of the Transwell device was then removed and the glioblastoma cells in the lower chamber were let to grow for 48 h further. Cytotoxicity on glioblastoma cells, produced by Dox permeated through hCMEC/D3 cells during the first 3 h, was measured at the end of this incubation period.

As it can be noted from Figure 7, after 3 h, Dox delivery in the medium of the lower chamber increases dose dependently: loading of Dox within SLN grants a higher delivery than free Dox.

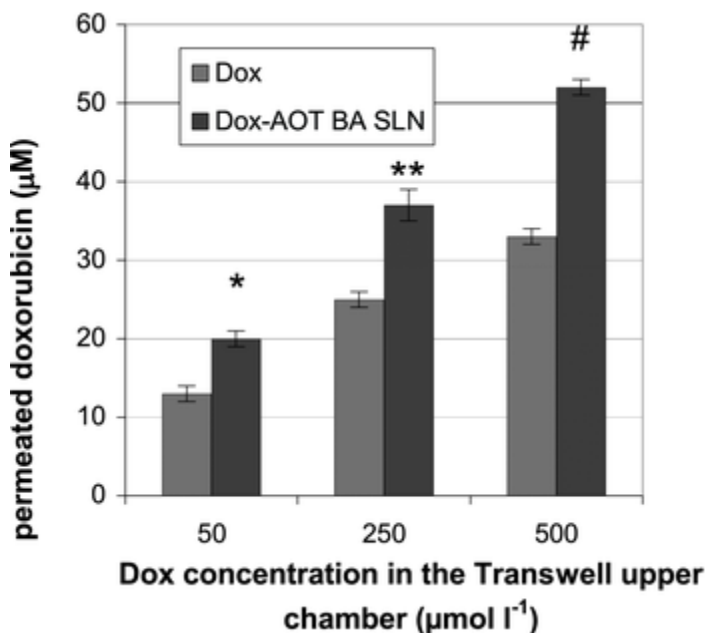


**Figure 7.**

- Open in figure viewer
- Download Powerpoint slide

Dox permeation through hCMEC/D3 cell monolayer from Dox aqueous solution and from Dox–AOT BA–SLN at 50, 250, 500  $\mu\text{M}$  Dox concentration after 3 h. Dox–AOT versus Dox: \*  $p < 0.02$ ; \*\*  $p < 0.005$ ; #  $p < 0.001$  ( $n = 3$ ).



The amount of free Dox that permeated through the hCMEC/D3 cell monolayer dose dependently decreased cell viability for CV17 and U87-MG cells (Figs. 8a and 8b), but had little effect on 01010627 cells (Fig. 8c). In keeping with the major permeation of Dox from Dox–AOT-loaded BA–SLN, such Dox formulation significantly reduced the cell viability in all the glioblastoma cell lines, resulting more effective than free Dox.

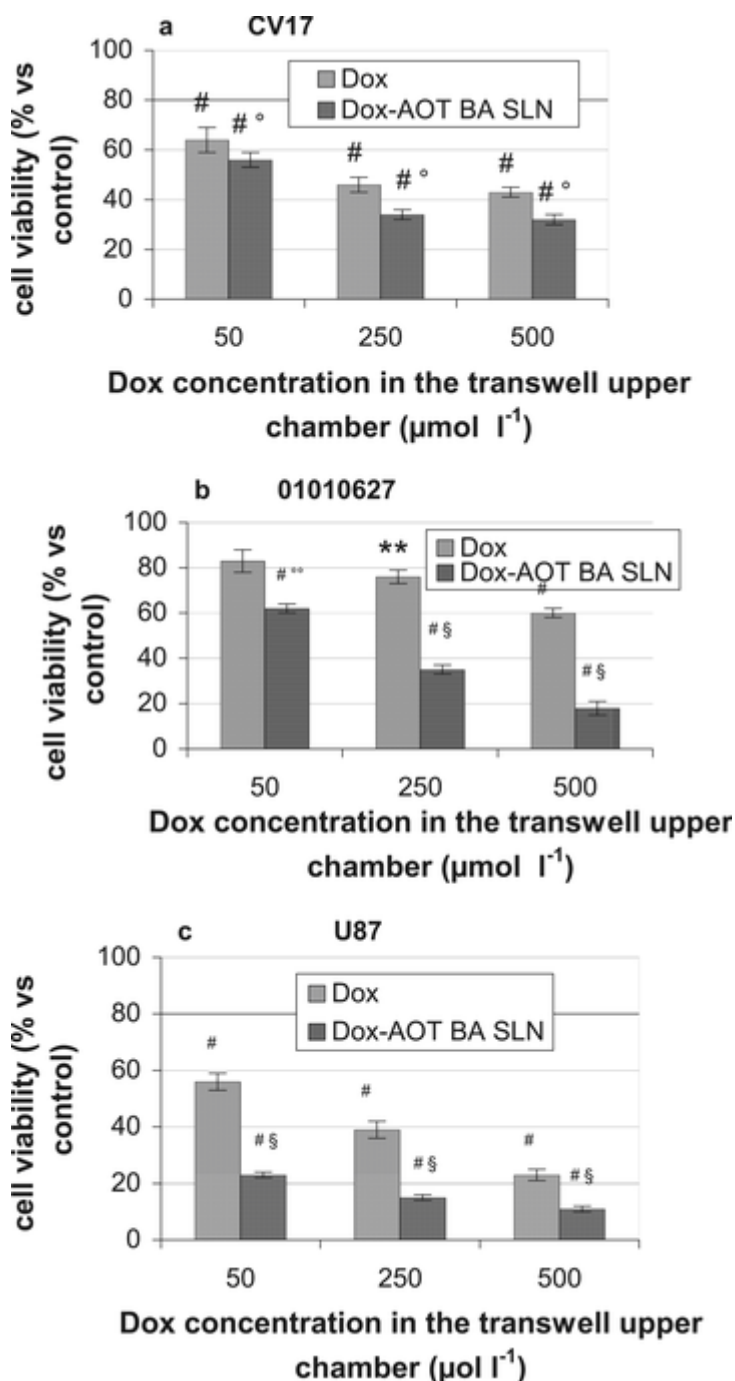


**Figure 8.**

- [Open in figure viewer](#)
- [Download Powerpoint slide](#)

Cytotoxicity of permeated Dox from Dox aqueous solution and from Dox–AOT BA–SLN on three human glioma cell lines: a, CV17; b, 01010627; c, U87. Significance versus untreated cells

(CTRL): \*  $p < 0.05$ ; \*\*  $p < 0.02$ ; #  $p < 0.001$ ; Dox–AOT versus Dox: °  $p < 0.05$ ; °°  $p < 0.02$ ; §  $p < 0.001$  ( $n = 4$ ).

## DISCUSSION

In this experimental work, Dox-loaded fatty acid SLN were obtained thanks to HIP between Dox and various anionic surfactants: despite its hydrophilic character, Dox can be entrapped in SLN, EE% being dependent on the surfactant used as counterion, with the best results obtained with AOT. HIP is a well-known technique used to “lyophilize” hydrophilic drugs[39]: based on the interaction of a surfactant and an opposite charged drug, HIP takes place at surfactant concentrations below the critical micelle concentration, leading to the precipitation of an insoluble electrostatic complex between the two molecules, with increased lipophilicity. The coacervation technique is an innovative method used to produce SLN and it has been coupled several times to HIP to encapsulate hydrophilic drugs.[22, 23, 40] Various lipid matrixes were used to prepare Dox–AOT-loaded SLN. Obtained EE% was similar among the various lipid matrixes: entrapment in the lipid matrix was confirmed by release experiments.

Behenic acid was chosen as lipid matrix, because, contrary to PA, it did not cause any detectable cytotoxicity against hCMEC/D3 cells used for permeation experiments. Permeation experiments were performed for 24 h because Dox–AOT-loaded SLN and free Dox did not cause any important cytotoxicity to hCMEC/D3 cells within this period of time. Entrapment in SLN caused an increase in permeation of Dox through hCMEC/D3 cell monolayer.

Doxorubicin also maintained its cytotoxicity against glioma cells if entrapped in SLN. Indeed, although Dox is highly cytotoxic against glioblastoma cells *in vitro*, [41] its clinical use is hampered by its low delivery across BBB. The abundance of tight and adherent junctions, the lack of fenestrations, the presence of several drug efflux transporters on the luminal side of BBB, such as Pgp, MRP-1, -2, and -4 and breast cancer-resistance protein (BCRP), are majorly responsible for the poor drug delivery across BBB.[42] hCMEC/D3 cells, as well as primary human BBB cells, are known to express Pgp and BCRP on their luminal side[43]; these two transporters actively efflux Dox back in the bloodstream.[42] BBB is disrupted in the bulk core of glioblastoma, but it is intact in the so-called brain adjacent to tumor (BAT) area, where isolated glioblastoma cells, hard to eradicate by surgery or radiotherapy, may find a favorable niche to grow and disseminate.[42] The presence of the intact BBB makes Dox hardly delivered to BAT area. To overcome this limitations, several alternative formulations of Dox, for example, liposome- and nanoparticle-based formulation[41, 44-46] have been produced. The present work shows a new formulation of Dox that can be a valid tool to permeate BBB monolayer, because Dox–AOT-loaded SLN achieved a higher delivery of the drug across the BBB, without any increase of toxicity on BBB cells compared with the free drug. Uptake experiments showed that Dox–AOT BA–SLN enter within BBB cells in a dose-dependent manner, suggesting that SLN were effective tools to deliver Dox across BBB monolayer through a transcytotic pathway. By contrast, Dox uptake remained lower and did not change after increasing the drug concentration, confirming the poor permeability of the drug in our model, as it occurs in most BBB models. More importantly, Dox–AOT-loaded SLN had a superimposable cytotoxicity to Dox on isolated glioblastoma cells and higher cytotoxicity than free Dox on glioblastoma cells cultured under BBB monolayer. Such increase could be because of the higher permeation of Dox–AOT-loaded SLN through the hCMEC/D3 cell monolayer.

Glioblastoma cell lines may differ for the sensitivity to Dox, for instance, in these experimental conditions, 01010627 were significantly less sensitive than CV17 and U87-MG. Such difference reflects the higher variability of primary glioblastoma samples, which may widely differ for the protein involved in Dox efflux, such as Pgp, MRP-1, and BCRP,[47] DNA repairing systems,

proapoptotic. or prosurvival proteins.[48] All these factors may account for the different response to Dox-free drug. Noteworthy is the fact that the efficacy of Dox–AOT-loaded SLN is higher than that of free drug and shows less variability among each glioblastoma cell line in coculture systems. We can speculate that the higher drug delivery granted by SLN allows Dox to reach a concentration sufficiently higher to overcome most of these potential factors of resistance.

## CONCLUSIONS

Doxorubicin was entrapped in fatty acid SLN prepared through coacervation technique, thanks to HIP with negatively charged surfactants, used as counterions: in particular, AOT allowed a good EE% of Dox within SLN. BA–SLN showed no toxicity toward hCMEC/D3 cells, so Dox–AOT-loaded SLN were employed to study drug permeation through hCMEC/D3 cells monolayer, assumed as the *in vitro* model of the BBB. Entrapment in BA–SLN caused an increase in the permeation of Dox through hCMEC/D3 cells monolayer, whereas it did not affect the cytotoxicity toward three types of human glioblastoma cells. Moreover in coculture experiments with hCMEC/D3 and glioblastoma cells, it was demonstrated that, when delivered in SLN, Dox increased its cytotoxicity toward glioblastoma cells, because of its increased permeation through the endothelial cell monolayer.

According to these results, Dox–AOT-loaded BA–SLN proved to be a promising drug delivery system to enhance Dox brain uptake. Further *in vivo* studies are needed to confirm the suitability of SLN in enhancing Dox overcoming of the BBB.

## ACKNOWLEDGMENTS

The authors wish to acknowledge Compagnia di San Paolo, under the research project “Development of solid lipid nanoparticles (SLN) as vehicles of antineoplastic drugs to improve the pharmacological glioblastoma therapy” (ORTO11WINST).

## REFERENCES

- 1Davson H, Segal M. 1996. Physiology of the CSF and blood–brain barrier. Boca Raton, Florida: CRC Press:
- 2Begley DJ. 1996. The blood–brain barrier: Principles for targeting peptides and drugs to the central nervous system. *J Pharm Pharmacol* 48:136–146.
- 3Dallas S, Miller DS, Bendayan R. 2006. Multidrug resistance-associated proteins: Expression and function in the central nervous system. *Pharmacol Rev* 58:140–161.
- 4Rapoport IR. 2000. Osmotic opening of the blood–brain barrier: Principles, mechanism, and therapeutic applications. *Cell Mol Neurobiol* 20:217–230.
- 5Lai F, Fadda AM, Sinico C. 2013. Liposomes for brain delivery. *Expert Opin Drug Deliv* 10:1003–1022.
- 6Kreuter J. 2002. Transport of drugs across the blood–brain barrier by nanoparticles. *Curr Med Chem* 2:241–249.
- 7Patil SA, Patil R, Miller DD. 2013. Large conductance, calcium activated potassium (BK) channels as new therapeutic target for glioma. *Int J Bioorg Chem Mol Biol* 1:1–2.
- 8Omuro A, De Angelis LM. 2013. Glioblastoma and other malignant gliomas. A clinical review. *JAMA* 10:1842–1850.
- 9Schiffer D, Annovazzi L, Caldera V, Mellai M. 2010. On the origin and growth of gliomas. *Anticancer Res* 30:1977–1998.

- 10 Wohlfart S, Gelperina S, Kreuter J. 2012. Transport of drugs across the blood–brain barrier by nanoparticles. *J Control Release* 161:264–273.
- 11 De Rosa G, Salzano G, Caraglia M, Abbruzzese A. 2012. Nanotechnologies: A strategy to overcome blood–brain barrier. *Curr Drug Metab* 13:61–69.
- 12 Müller RH, Mäder K, Gohla S. 2000. Solid lipid nanoparticles (SLN) for controlled drug delivery—A review of the state of the art. *Eur J Pharm Biopharm* 50:161–177.
- 13 Müller RH, Lucks JS. 1996. Patent EUR06055497.
- 14 Gasco MR. 1993. Patent US5250236.
- 15 Mumper RJ, Jay M. 2006. Patent US7153525.
- 16 Siekmann B, Westesen K. 1994. Thermoanalysis of the recrystallization process of melt-homogenized glyceride nanoparticles. *Colloid Surf B* 3:159–175.
- 17 Schubert MA, Müller-Goymann CC. 2003. Solvent injection as a new approach for manufacturing lipid nanoparticles—Evaluation of the method and process parameters. *Eur J Pharm Biopharm* 55:125–131.
- 18 Gallarate M, Trotta M, Battaglia L, Chirio D. 2009. Preparation of solid lipid nanoparticles from w/o/w emulsions: Preliminary studies on insulin encapsulation. *J Microencaps* 26:394–402.
- 19 Trotta M, Cavalli R, Carlotti ME, Battaglia L, Debernardi F. 2005. Solid lipid micro-particles carrying insulin formed by solvent-in-water emulsion-diffusion technique. *Int J Pharm* 288:281–288.
- 20 Battaglia L, Trotta M, Gallarate M, Carlotti ME, Zara GP, Bargoni A. 2007. Solvent lipid nanoparticles formed by solvent-in-water emulsion diffusion technique: Development and influence of insulin stability. *J Microencaps* 14:672–684.
- 21 Battaglia L, Gallarate M, Cavalli R, Trotta M. 2010. Solid lipid nanoparticles produced through a coacervation method. *J Microencaps* 27:78–85.
- 22 Gallarate M, Trotta M, Battaglia L, Chirio D. 2010. Cisplatin loaded SLN produced by coacervation technique. *J Drug Del Sci Tech* 20:343–347.
- 23 Gallarate M, Battaglia L, Peira E, Trotta M. 2011. Peptide-loaded solid lipid nanoparticles prepared through coacervation technique. *Int J Chem Eng*.
- 24 Wong HL, Bendayan R, Rauth AM, Li Y, Wu XY. 2007. Chemotherapy with anticancer drugs encapsulated in solid lipid nanoparticles. *Adv Drug Deliv Rev* 59:491–504.
- 25 Hong Y, Jing M, Yong-Zhong D, Jian Y, Fu-Qiang H, Su Z. 2008. Cellular uptake of solid lipid nanoparticles and cytotoxicity of encapsulated paclitaxel in A549 cancer cells. *Int J Pharm* 348:137–145.
- 26 Teskac K, Kristl J. 2010. The evidence for solid lipid nanoparticles mediated cell uptake of resveratrol. *Int J Pharm* 390:61–69.
- 27 Tacar O, Sriamornsak P, Dassa CR. 2013. Doxorubicin: An update on anticancer molecular action, toxicity and novel drug delivery systems. *J Pharm Pharmacol* 65:157–170.
- 28 Li X, Ding LY, Xub Y, Wang Y, Ping Q. 2009. Targeted delivery of doxorubicin using stealth liposomes modified with transferring. *Int J Pharm* 373:116–123.
- 29 Park J, Fong PM, Lu J, Russel KS, Booth CJ, Saltzman WM, Fahmy TM. 2009. PEGylated PLGA nanoparticles for the improved delivery of doxorubicin. *Nanomedicine* 5:410–418.
- 30 Bhattacharjee J, Verma G, Aswal VK, Hassan PA. 2008. Small angle neutron scattering study of doxorubicin–surfactant complexes encapsulated in block copolymer micelles. *Pramana* 71:991–995.
- 31 Jennings V, Schäfer-Korting M, Gohla S. 2000. Vitamin A-loaded solid lipid nanoparticles for topical use: Drug release properties. *J Control Release* 66:115–126.
- 32 Monnaert V, Betbeder D, Fenart L, Bricout H, Lenfant AM, Landry C, Cecchelli R, Monflier E, Tilloyet S. 2014. Effects of  $\gamma$ - and hydroxypropyl- $\gamma$ -cyclodextrins on the

- transport of doxorubicin across an in vitro model of blood–brain barrier. *J Pharmacol Exp Ther* 311:1115–1120.
- 33Pinzón-Daza ML, Garzón R, Couraud PO, Romero IA, Weksler B, Ghigo D, Bosia A, Riganti C. 2012. The association of statins plus LDL receptor-targeted liposome-encapsulated doxorubicin increases in vitro drug delivery across blood–brain barrier cells. *Brit J Pharmacol* 167:1431–1447.
  - 34Riganti C, Salaroglio IC, Pinzón-Daza ML, Caldera V, Campia I, Kopecka J, Mellai M, Annovazzi L, Couraud PO, Bosia A, Ghigo D, Schiffer D. 2014. Temozolomide down-regulates P-glycoprotein in human blood–brain barrier cells by disrupting Wnt3 signaling. *Cell Mol Life Sci* 71:499–516.
  - 35Weksler BB, Subileau EA, Perrière N, Charneau P, Holloway K, Leveque M, Tricoire-Leignel H, Nicotra A, Bourdoulous S, Turowski P, Male DK, Roux F, Greenwood J, Romero IA, Couraud PO. 2005. Blood–brain barrier-specific properties of a human adult brain endothelial cell line. *FASEB J* 19:1872–1874.
  - 36Siflinger-Birnboim A, Del Vecchio PJ, Cooper JA, Blumenstock FA, Shepard JM, Malik AB. 1987. Molecular sieving characteristics of the cultured endothelial monolayer. *J Cell Physiol* 132:111–117.
  - 37Westesen K, Bunjes H, Koch MHJ. 1997. Physicochemical characterisation of lipid nanoparticles and evaluation of their drug loading capacity and sustained release potential. *J Control Release* 48:223–236.
  - 38Guangli W, Shuhua X, Duanyun S, Changxiao L. 2008. Improved HPLC method for doxorubicin quantification in rat plasma to study the pharmacokinetics of micelle encapsulated and liposome-encapsulated doxorubicin formulations. *Biomed Chromatogr* 22:1252–1258.
  - 39Meyer JD, Manning MC. 1998. Hydrophobic ion pairing: Altering the solubility properties of biomolecules. *Pharm Res* 15:188–193.
  - 40Battaglia L, Serpe L, Muntoni E, Zara GP, Trotta M, Gallarate M. 2011. Methotrexate-loaded SLNs prepared by coacervation technique: In vitro cytotoxicity and in vivo pharmacokinetics and biodistribution. *Nanomedicine (Lond.)* 6:1561–1573.
  - 41Hau P, Fabel K, Baumgart U, Rummele P, Grauer O, Bock A, Dietmaier C, Dietmaier W, Dietrich J, Dudel C, Hubner F, Jaucj T, Drechsel E, Kleiter I, Wismeth C, Zellner A, Brawanski A, Steinbrecher A, Marienhagen J, Bogdahan U. 2004. Pegylated liposomal doxorubicin-efficacy in patients with recurrent high-grade glioma. *Cancer* 100:1199–1207.
  - 42Agarwal S, Sane R, Oberoi R, Ohlfest JR, Elmquis WF. 2011. Delivery of molecularly targeted therapy to malignant glioma, a disease of the whole brain. *Expert Rev Mol Med* 13:e17.
  - 43Tai LM, Loughlin AJ, Male DK, Romero IA. 2009. P-glycoprotein and breast cancer resistance protein restrict apical-to-basolateral permeability of human brain endothelium to amyloid- $\beta$ . *J Cereb Blood Flow Metab* 29:1079–1083.
  - 44Ananda S, Nowak AK, Cher L, Dowling A, Brown C, Simes J, Rosenthal MA; the Cooperative Trials Group for Neuro-Oncology (COGNO). 2011. Phase 2 trial of temozolomide and pegylated liposomal doxorubicin in the treatment of patients with glioblastoma multiforme following concurrent radiotherapy and chemotherapy. *J Clin Neurosci* 18:1444–1448.
  - 45Steiniger SC, Kreuter J, Khalansky AS, Skidan IN, Bobruskin AI, Smirnova ZS, Severin SE, Uhl R, Kock M, Geiger KD, Gelperina SE. 2004. Chemotherapy of glioblastoma in rats using doxorubicin-loaded nanoparticles. *Int J Cancer* 109:759–767.
  - 46Wohlfart S, Khalansky AS, Gelperina S, Begley D, Kreuter J. 2011. Kinetics of transport of doxorubicin bound to nanoparticles across the blood–brain barrier. *J Control Release* 154:103–107.

- 47Riganti C, Salaroglio IC, Caldera V, Campia I, Kopecka J, Mellai M, Annovazzi L, Bosia A, Ghigo D, Schiffer D. 2013. Temozolomide downregulates P-glycoprotein expression in glioblastoma stem cells by interfering with the Wnt3a/GSK3/ $\beta$ -catenin pathway. *Neuro Oncol* 15:1502–1517.
- 48Bai RY, Staedke V, Riggins GJ. 2011. Molecular targeting of GBM: Drug discovery and therapies. *Trends Mol Med* 17:301–312.